A Study of the Behavior of Boron Diffusion in Plain Carbon Steels

L.L. Qian and G.A. Stone

Boronizing treatment of ferrous materials has been widely employed by industry as a surface-strengthening technology for inhibition of corrosion, wear, and erosion. Pack boronization using a pack composition that produces a graded boride microstructure has been studied using AISI 1018 and 1045 steels. Carbon in these alloys creates a resistance to boron diffusion because a carbon-enriched zone forms in front of the boride layer.

The carbon concentration at the boride/pearlite interface was found to be as high as 3.0% in AISI 1045 steel. No significant layer phenomena could be distinguished inside the boron layer using the pack composition developed during this research. This result is significant because a graded microstructure with a continuous variation of the boron composition has been produced. Evidence developed during this study suggests that the boride layer consists of a mixture of FeB, Fe_2B, and FeB_x, which is probably FeB_{19}. Analysis determined a measure of the resistance of carbon to boron diffusion at the boride/pearlite interface.

Keywords

diffusion, alloying effects, boron, carbon steel, SEM, mathematical model

1. Introduction

BORIDING TREATMENT of ferrous materials is applicable in a wide range of industrial applications. The boride layer formed has the properties of high melting point, high metallic resistivity, and high hardness. Recent studies have found that boride coatings have potential as protective coatings in corrosion environments (Ref 1). Boriding is also an effective method of surface hardening and is used worldwide to combat wear and erosion (Ref 2, 3). Some of the important achievements are that:

- The average service life of forging dies in a wide range of sizes has been increased up to ten times by boronizing.
- The life of pipes that were worn out by vinyl-chloride-containing traces of hydrochloric acid in a polyvinyl chloride plant was increased from half a year to two years after boriding.
- High-alloy tool steels, used as the clamping jaw material for mechanical testing machines, were replaced by simple borided materials, reducing materials and production costs while increasing the number of load cycles withstood by the clamping jaw.
- High abrasive wear resistance, over a prolonged period, has been achieved in diesel engine drive gears by boriding technology.
- The service life of borided burner nozzles, swirl elements, and injector tops in chemical plants is two to three times longer than that of unborided parts (Ref 2).

L. Qian and **G.A. Stone,** Department of Metallurgical Engineering, South Dakota School of Mines & Technology, 501 East Saint Joseph Street, Rapid City, SD 57701-3995, USA, gstone@silver.sdsmt.edu.

Boride coatings have been achieved by gas boronizing agents, liquid boronizing compounds, and pack cementation with solid powders (Ref 4, 5). The solid pack method seems to be the most popular, probably due to the economics of the process and its wide applicability. This study utilized pack boriding technology.

2. Experimental Approach

The object of the work was to study boron diffusion behavior in plain carbon steel and, in retrospect, describe it by introducing a coefficient into a conventional solution of Fick's second law. To accomplish this task, structural and composition data were collected using scanning electron microscopy (SEM) and energy-dispersive x-ray spectrometry (EDX). Quantitative metallography and computer simulation techniques were also used.

The pack composition used in this study was developed by Madhusudan (Ref 6). The samples used in this study are listed in Table 1.

Table 1 Borided samples used in this study

No.	Material	Boriding temperature, °C	Duration, h
1	AISI 1018	900	4
2	AISI 1018	900	6
3	AISI 1018	900	8
4	AISI 1018	900	10
5	AISI 1045	900	4
6	AISI 1045	900	6
7	AISI 1045	900	8
8	AISI 1045	900	10
9	AISI 1018	975	4
10	AISI 1045	975	4

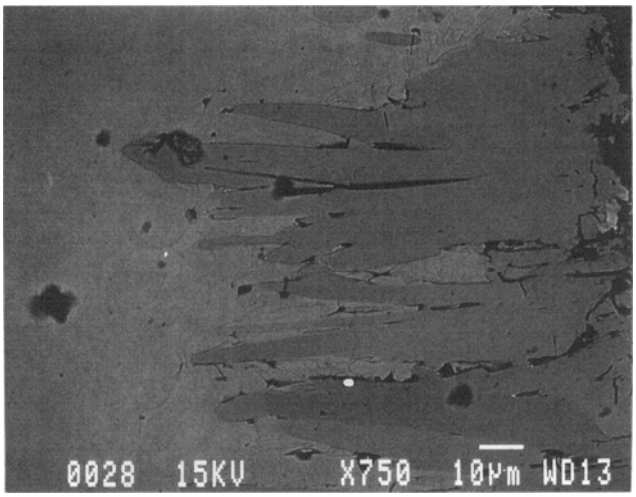

Fig. 1 Backscattered SEM image of AISI 1045 steel sample that was borided at 900 °C for 8 h

3. Experimental Results and Discussion

3.1 *Constitution of Boride Layer*

Experimental evidence shows that there is not only FeB and Fe_2B but also FeB_x in the boride layer. No distinguishable phase layer can be identified inside the boride layer. The stoichiometry appears to change as a function of distance through the boride layer. It is believed that the volume fraction of a new phase, possibly FeB_{19}, increases as a function of distance, giving the appearance of a change in stoichiometry.

Figure 1 is a backscattered SEM image of an AISI 1045 sample that was borided at 900 °C for 8 h. From this figure it can be seen that the brightness varies along the needle, which can be interpreted as the boron concentration varying along the needle. This indicates that a combination of FeB, FeB_x, and Fe_2B inside the boriding layer is possible.

Electron probe microanalysis shows that the relative x-ray fluorescent intensity of iron increases smoothly from the surface toward the core of the sample (Ref 7). A continuous variation of boron content is observed. On the other hand, boron content is much higher than 0.162 wt% (the boron content of FeB) from the surface up to about 50 to 60 µm. This supports the idea that a mixture of FeB and FeB_x exists in this area. The absence of particular phase or layer phenomena is very interesting. Transmission electron microscopy studies are planned to resolve the details of the microstructure.

According to the B-Fe phase diagram (Ref 8), the equilibrium phases are α-Fe, ε (Fe_2B), ξ (FeB), η (FeB_{19}), and B. It is realized that under certain conditions, depending on boron concentration, boriding temperature, and time, it is possible for Fe_2B, FeB, and FeB_{19} to be present and for an FeB, FeB_{19} mixture to exist in a wide range of boron contents. This verifies theoretically that FeB_x could be FeB_{19}. However, there is a lack of knowledge about structure and properties of FeB_{19}, so it is difficult to identify the FeB_{19} phase by means of common experimental approaches. Even so, it is most likely that FeB_{19} does exist in the boride layer.

Table 2 Carbon content at each point in front of the boride layer, calculated by quantitative metallographic analysis for sample 8

Distance from the edge, µm	Carbon content, wt%
83.0	2.23
89.8	3.00
95.8	2.75
104.4	2.67
109.1	2.69
117.1	2.48
123.7	2.47
134.9	2.51

3.2 *Effect of Carbon*

In order to explore the effect of carbon on boron diffusion, a manual quantitative metallographic analysis was performed. Metallographic pictures were taken along a line in front of the boride needles at a magnification of 10,000×, using SEM. The fraction of the cementite in pearlite was measured and calculated by the P_p technique:

$$f_{Fe_3C} = P_p \quad \text{(Eq 1)}$$

where f_{Fe_3C} is the fraction of Fe_3C. According to the Lever rule and the Fe-C equilibrium phase diagram:

$$f_{Fe_3C} = \frac{X - 0.02}{6.69 - 0.02} \quad \text{(Eq 2)}$$

where X is the carbon content in Fe_3C. Substituting Eq 2 for Eq 1 yields:

$$X = 6.67\,P_p + 0.02 \quad \text{(Eq 3)}$$

where P_P is the number of points which fall in the cementite per total number of points, i.e. the point fraction of cementite. At 900 °C the equilibrium carbon content in iron (as Fe_3C) is about 1.2 wt.%. These samples were furnace cooled, so near-equilibrium conditions were expected. Because pearlite is expected to form from austenite at a composition of about $X = 0.8$ w/o carbon, the carbon content in the pearlite regions should be fixed. The carbon content in front of the needles in the boride layer is extremely high. These results, calculated by Eq 3, are presented in Table 2.

Previous research (Ref 9) has shown that the solubility of carbon in the boride layer is very limited. Therefore, carbon is driven out of the boride layer completely during the boron diffusion process. Dukarevich and Mozharov estimated that the amount of carbon in this zone is less than 0.005 wt% (Ref 9).

A computer program was written that accounted for the mass balance of carbon, in order to calculate the carbon profile in front of the boride layer. It shows that a reasonable carburized layer with a thickness estimated to be 51 times the thickness of the boride layer is produced (Ref 7). The result of the manual metallographic analysis is in good agreement with the

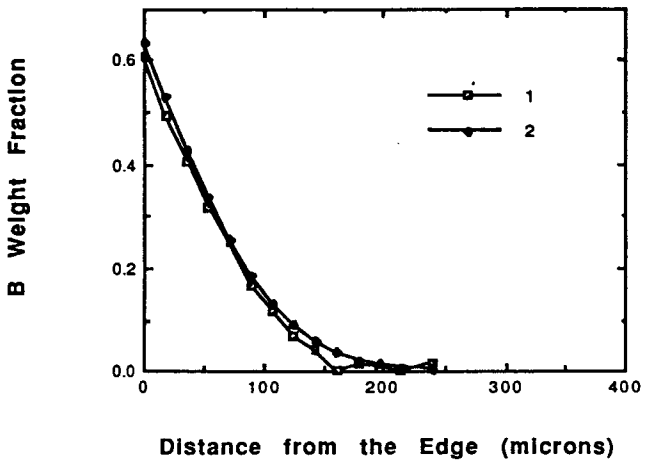

Fig. 2 Comparison of the distribution of boron weight fraction obtained from (1) experiment and (2) mathematical model (Eq 6 in text) using AISI 1018 steel that was borided at 900 °C for 10 h

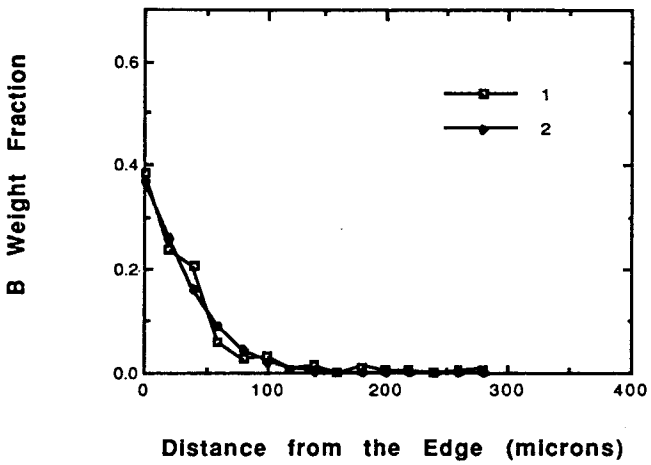

Fig. 3 Comparison of the distribution of boron weight fraction obtained from (1) experiment and (2) mathematical model (Eq 6 in text) using AISI 1045 steel that was borided at 900 °C for 4 h

profile of carbon concentration versus distance that was generated by the computer model.

At the boriding temperature, carbon atoms are rejected from the iron lattice and are pushed toward the core. This produced a carbon-enriched layer between the boride layer and the matrix. Carbon atoms diffuse much deeper into the matrix, resulting in a carburized layer much thicker than the boride layer. The diffusivity of carbon in γ-Fe is 2.886×10^{-11} m^2/s at 900 °C, which is higher by an order of two than the diffusivity of boron at the same temperature. This difference in diffusivity could be the reason why a much thicker layer of carburized zone forms. Because the solubility of carbon in iron is limited, carbides are formed when the limit of solubility is reached.

A pearlitic microstructure is observed adjacent to the boride layer. The high carbon content in the steel appears to have thickened the carbide phase in the pearlite. Other carbide precipitate morphologies were not observed.

Brakman et al. (Ref 10) indicated that the carbon driven out of the boride layer combines with boron to form borocementite. Unfortunately, the experimental techniques used in the present research are not able to identify the difference between $Fe_3(B,C)$ and Fe_3C.

The microhardness measurements reported by Madhusudan (Ref 6) showed that at a distance of about 60 μm from the surface the hardness was about 800 to 1000 HV. These values are typical of a carburized zone.

In a recent study, SEM micrographs of AISI 1018 and AISI 1045 steel showed that increasing the carbon content of steel greatly reduces the needle morphology of the borides (Ref 7). In AISI 1018, with lower carbon content, diffusion of boron is less hindered. The boride needles grow deeper into the matrix. In AISI 1045, with higher carbon content, the needle morphology is greatly reduced. The anisotropic nature of the boride lattice is reduced by the carbon dissolved in iron, so that the diffusion in preferred directions is avoided (Ref 10).

3.3 *Boron Content at the Sample Surface*

EDX provided a tool for measuring the boron content in the steels. According to the ZAF method (Ref 11):

$$C_{Fe} = [ZAF]_{(Fe)} \frac{I_{Fe}}{I_{(Fe)}} \qquad \text{(Eq 4)}$$

where Z is the atomic number factor, A is the absorption factor, and F is the characteristic fluorescence correction, and $C_B + C_{Fe} = 1$, where C_B is the boron weight fraction in the boride layer and CFe is iron weight fraction in this layer. The boron weight fraction can then be calculated experimentally:

$$C_B\text{-ex} = 1 - [ZAF]_{(Fe)} \frac{I_{Fe}}{I_{(Fe)}} \qquad \text{(Eq 5)}$$

where I_{Fe} and $I_{(Fe)}$ are the measured X-ray intensities of iron from the sample and the standard, where C_B-ex is the boron weight fraction as a function of distance, obtained from experimental data.

Values for the x-ray intensity of iron, at each point along a straight line that was normal to the surface of the sample, were collected step by step and were put into Eq 5. The experimental profiles of C_B-ex versus distance are curve 1 in Fig. 2 and curve 1 in Fig. 3. Curve 2 is the fit to Fick's second law, to be discussed in the next section.

EDX measurements show that relative x-ray intensity of iron is extremely low at the surface of the sample (Ref 7). That means the boron content is very high from the surface of the sample up to about 50 μm toward the center. It can be seen that the surface content of boron is variable during the boriding treatment. It tends to increase as the time of boride treatment increases, and it may be affected by temperature or unknown variables. Estimation of the amount of boron in the surface is a very complicated problem, because there is no way to measure how the surface concentration changes. It is therefore necessary to assume equilibrium as a first approximation. However, experimental results suggest that the system is not at equilibrium.

3.4 *Mathematical Diffusion Model*

The average weight fraction of boron at the surface of the sample, C_s, is a function of temperature, time, and other variables determined by the computer model. Although carbon has significant effects on the behavior of boron diffusion, there is little information about the boundary condition C_s and the diffusivity of boron in Fe-C. In order to find a mathematical fit, two computer programs were written (Ref 7). The first program prepares a data file that serves as the input of the second program. It is specially designed to process a large amount of experimental data in a very easy and quick way. The second program determines the acceptable mathematical model by testing a variety of different possible mathematical expressions. At the same time, it calculates the boron weight fraction, C_B-ex, from experimental data. The result of the computer programs is a modified diffusion model of Fick's second law:

$$C(X,t) = C_s(t, ...)\left[1 - \text{erf}\left(\frac{X}{2\sqrt{D/q^2}\sqrt{t}}\right)\right] \quad \text{(Eq 6)}$$

where $C(X,t)$ is the weight fraction of boron, the function of X and t; X is the vertical distance from the surface of the sample; t is the time of boriding; erf is error function; D is the diffusivity of boron; and q = 1.5 at 900 °C, a measure of the resistance of carbon to boron diffusion at the boride/pearlite interface. This coefficient was determined by the computer program.

The values of C_s determined by the computer model are 0.37, 0.44, 0.49, and 0.64, corresponding to the diffusion times of 4, 6, 8, and 10 h, respectively. Results show that these values succeed for all the samples except sample 6 (Ref 7).

The mathematical model and experimental data are compared in Fig. 2 and 3. This model is in good agreement with the boron weight fraction distribution from experimental measurements in all the samples (Ref 7).

4. Conclusions

- The content of boron at the surface of the samples is a variable. It is a function of boriding time and other unknown variables. The regularity of changing surface content is believed to depend on the composition of a mixture of the ξ (FeB) and η (FeB_{19}) phases.
- The constitution in the boride layer is a mixture of FeB, Fe_2B, and FeB_x. The content of FeB_x is believed to decrease gradually from the surface to the core within the boride layer. FeB_x cannot be distinguished by the present study, but it is most likely FeB_{19}.
- Carbon has a strong influence on boron diffusion in steel. A carbon-enriched zone is formed underneath the boride layer. The maximum measured carbon content is as high as 2.2 to 3.0 wt% in AISI 1045 steel borided at 900 °C for 10 h. This is in excess of the carbon content suggested by the phase diagram. It is expected that carbide particles would form under equilibrium conditions. However, no carbide particles are present at the interface. It is concluded, then, that the excess carbon produces a thickening of the cementite in the pearlitic structure. This has been confirmed through direct metallographic measurements.
- By obtaining an average surface boron concentration, $C_S(t, ...)$, and forcing a fit to Fick's second law solution of a semi-infinite bar, which is modified by introducing the parameter q, all the experimental data, with the one noted exception, can be modeled by Eq 6.
- The result is significant because a single-layer microstructure with a continuous variation of the boron composition has been produced. No distinguishable phases formed in the layer. This solves the original problem of mechanically incompatible FeB and Fe_2B phases that may cause spalling at the FeB/Fe_2B interface, and a stronger boronized surface layer can be provided.

Acknowledgment

The authors are grateful for the partial funding of this research through the State of South Dakota EPSCoR project, funded by grants from the National Science Foundation (EHR-9108773).

References

1. L.S. Lyakhovich and S.S. Bragilevskaya, Effects of Boriding on the Oxidation Resistance of Steel, *Protective Coatings on Metals*, Vol 2, G.V. Samsonov, Ed., Consultants Bureau, 1969, p 123-127
2. W. Fichtl, Boronizing and Its Practical Applications, *Mater Eng.*, Vol 2, 1981, p 276-286
3. R.H. Biddulph, Boronizing for Erosion Resistance, *Thin Solid Films*, Vol 45, 1977, p 341-347
4. D.N. Tsipas and C. Perez-Perez, A Boronizing Treatment for Low-Carbon Steels, *J. Mater Sci. Lett.*, Vol 1, 1982, p 298-299
5. P. Goeriot, F. Thevenot, and J.H. Driver, Surface Treatment of Steel: Borudif, A New Boriding Process, *Thin Solid Films*, Vol 78, 1981, p 67-76
6. S.R. Madhusudan, "Boriding of Steels," M.S. thesis, South Dakota School of Mines & Technology, 1992
7. L. Qian, "A Study of the Behavior of Boron Diffusion in Plain Carbon Steel," M.S. thesis, South Dakota School of Mines & Technology, 1993
8. Metallography, Structures and Phase Diagrams, Vol 8, 8th ed., *Metals Handbook*, American Society for Metals, 1973, p 270-272
9. I.S. Dukarevich and M.V. Mozharov, A Radioactive Isotope Study of Carbon Redistribution in the Borided Layer, *Protective Coatings on Metals*, Vol 4, G.V. Samsonov, Ed., Consultants Bureau, 1969, p 31-33
10. C.M. Brakman, A.W.J. Gommers, and E.I. Mittemaijir, Boriding Fe and Fe-C, Fe-Cr and Fe-Ni Alloys: Boride-Layer Growth Kinetics, *J. Mater Res.*, Vol 4 (No. 6), 1989, p 1354-1370
11. J.I. Goldstein, D.E. Newbury, P. Echlin, D.C. Joy, C. Fiori, and E. Lifshin, *Scanning Electron Microscopy and X-Ray Microanalyis: A Text for Biologists, Materials Scientists, and Geologists*, Plenum Press, 1981, p 306